Supporting Information

Real-time Observing Ultrafast Carrier and Phonon Dynamics in Colloidal Tin Chalcogenide van der Waals Nanosheets

Xufeng Li[1], Nannan Luo[2], Yuzhong Chen[1], Xiaolong Zou[2], Haiming Zhu[1,3]*

1. Centre for Chemistry of High-Performance & Novel Materials, Department of Chemistry, Zhejiang University, Hangzhou, Zhejiang, 310027, China

2. The Low-Dimensional Materials and Devices Laboratory, Tsinghua-Berkeley Shenzhen Institute, Tsinghua University, Shenzhen, Guangdong 518055, China

3. State Key Laboratory of Modern Optical Instrumentation, Zhejiang University, Hangzhou, Zhejiang, 310027, China.

* Email: hmzhu@zju.edu.cn

Contents

SI1. Morphology control of $SnSe_2$ nanoparticle

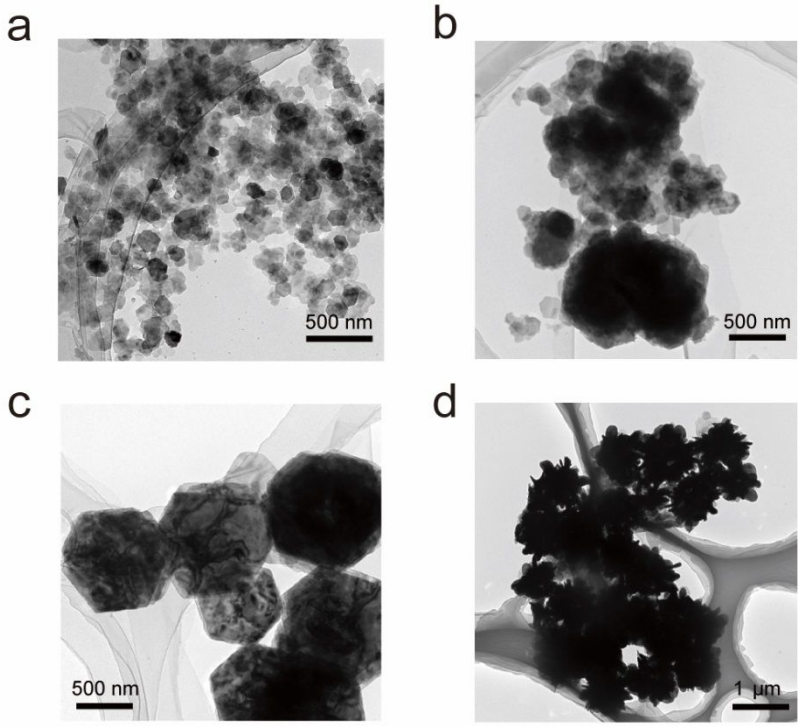

Fig. S1. $SnSe_2$ nanoparticle synthesized at different reaction condition. The lateral size of $SnSe_2$ NSs can be controlled by adjusting the radio of Sn and Se precursors. (a) Sn/Se=1/2, lateral size about 50-200 nm. (b) Sn/Se=1/3, lateral size about 200-500 nm. (c) Sn/Se=1/4, lateral size about 1-2 μm. If no morphology control agent Phen added into reaction system, the product will change to nanoflowers (d). This result is similar to the Li L et al's previous work.[1]

SI2. Thickness characterization

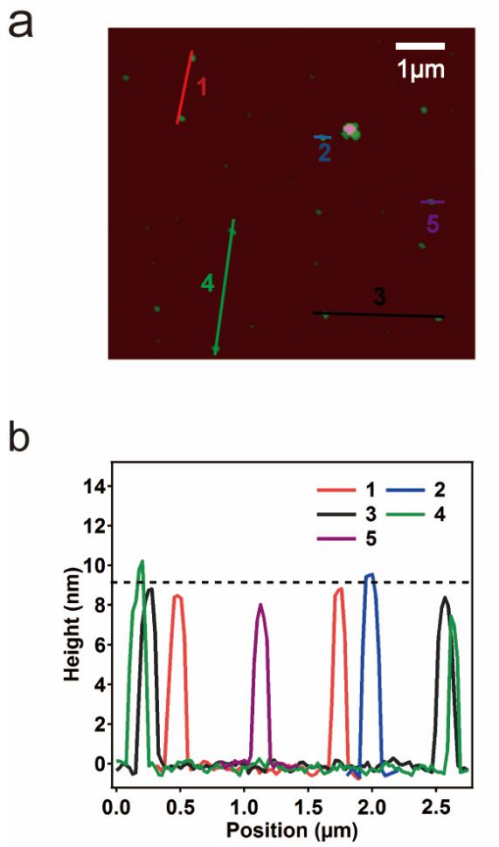

Fig. S2. Typical AFM image (a) and the height data (b) of $SnSe_2$ NSs. The morphology of $SnSe_2$ NSs in AFM image is similar to that in TEM image, and the single sheet which can be easily separated by spin-coating for AFM characterization shows the uniform thickness of ~9 nm.

SI3. Effective mass

Electron effective mass /m_e		Hole effective mass /m_e
Γ point：	M point：	Γ-K： 1.4
Γ-K： 0.1	M-Γ: 1.3	
Γ-M： 0.1	M-K: 0.6	

Tab. S1 Effective Mass of Carriers in $SnSe_2$ Band Structure by DFT

SI4. More data of 2.38 eV (520 nm) excitation

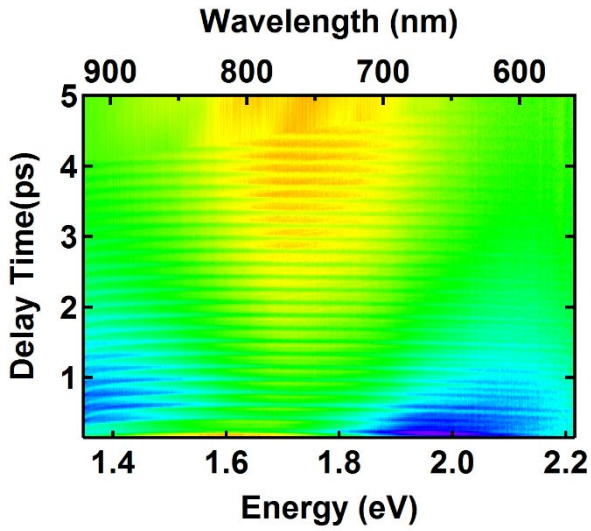

Fig. S3. Color plot of TA spectra after 2.38 eV (520 nm) excitation with linear delay time for details of oscillation pattern.

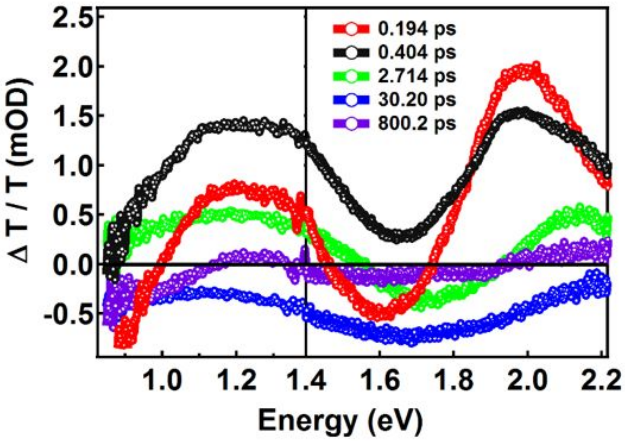

Fig. S4. TA spectra evolution at various pump-probe delays after 2.38 eV excitation.

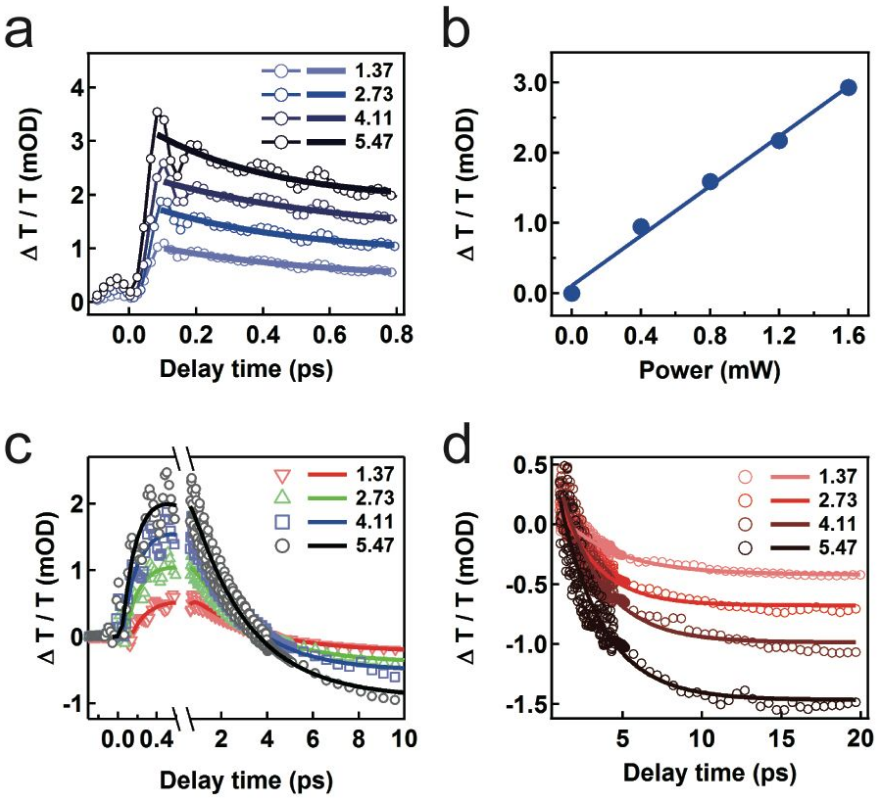

Fig. S5. Kinetics power-dependence ($\times 10^3$ mW/cm^2) after 2.38 eV (520 nm) excitation. The marks are experimental data and the solid lines are their exponential fits. (a) Decay kinetics of T_2 at different excitation power. (b) Signal intensity of T_2 at different excitation power. (c) Kinetics of T_1 at different excitation power. (d) Generation kinetics of PA at different power. All fitting life times are showed in Table S2.

Tab. S2 Fitting lifetimes of kinetics after 2.38 eV excitation

Signal	Power	Process	life time
T_2	0.4mW	decay	0.524±0.170ps
	0.8mW	decay	0.427±0.154ps
	1.2mW	decay	0.570±0.363ps
	1.6mW	decay	0.466±0.158ps
T_1	0.4mW	generate	0.217±0.030ps
		decay	2.812±0.212ps
	0.8mW	generate	0.219±0.030ps
		decay	2.501±0.167ps
	1.2mW	generate	0.231±0.031ps
		decay	2.492±0.152ps
	1.6mW	generate	0.194?0.030ps
		decay	2.539±0.169ps
PA	0.4mW	generate	2.726±0.166ps
		decay	448.7±10.7ps
	0.8mW	generate	2.686±0.149ps
		decay	501.94±19.1ps
	1.2mW	generate	2.403±0.142ps
		decay	486.35±15.5ps
	1.6mW	generate	2.864±0.35ps
		decay	520.2±20.2ps

SI5. More data of 1.45 eV (850 nm) excitation

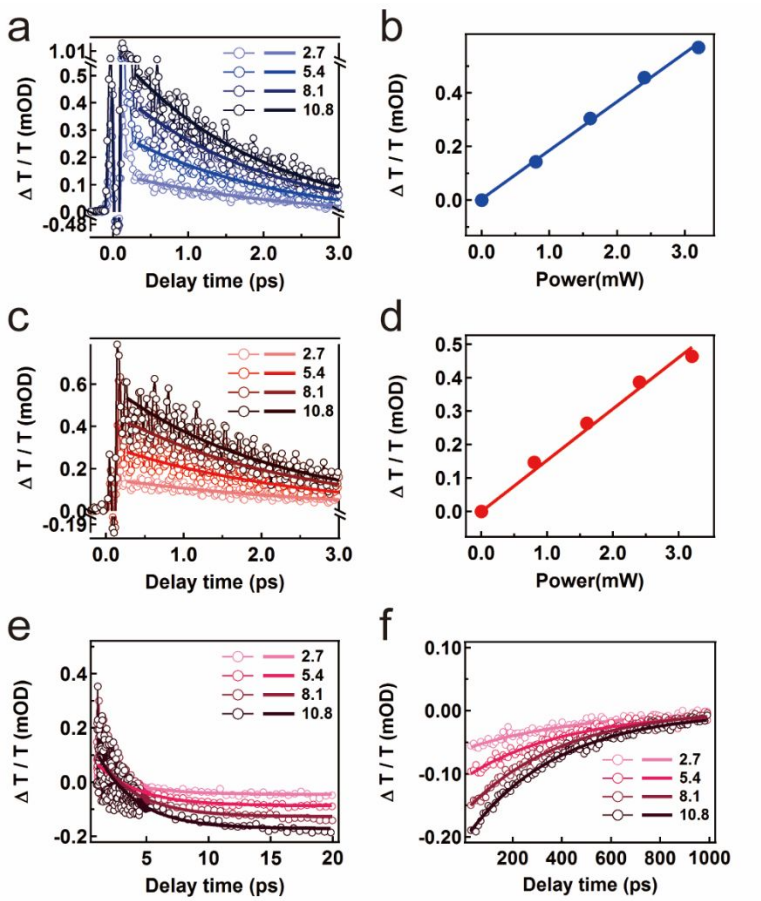

Figure S6. Kinetics power-dependence ($\times 10^3$ mW/cm^2) after 1.45 eV (850 nm) excitation. (a) Decay kinetics of T_2 at different excitation power. (b) Signal intensity of T_2 at different excitation power. (c) Decay kinetics of T_1 at different excitation power. (d) Signal intensity of T_1 at different excitation power. (e) Generation kinetics of PA at different excitation power. (f) Decay kinetics of PA at different excitation power. All fitting life times are showed in Table S3.

Tab. S3 Fitting life times of kinetics by 1.45 eV excitation

Signal	Power	Process	life time
B_2	0.8mW	decay	2.457±0.079ps
	1.6mW	decay	2.391±0.072ps
	2.4mW	decay	2.452±0.071ps
	3.2mW	decay	2.362±0.067ps
B_1	0.8mW	decay	3.643±0.165ps
	1.6mW	decay	3.415±0.148ps
	2.4mW	decay	3.386±0.142ps
	3.2mW	decay	3.278±0.129ps
A	0.8mW	generate	3.447±0.416ps
		decay	470.61±73.8ps

	1.6mW	generate	3.318±0.402ps
		decay	448.36±30.3ps
	2.4mW	generate	3.198±0.399ps
		decay	391.49±18.6ps
	3.2mW	generate	3.158±0.352ps
		decay	397.46±13.4ps

SI6. More data on coherent phonon

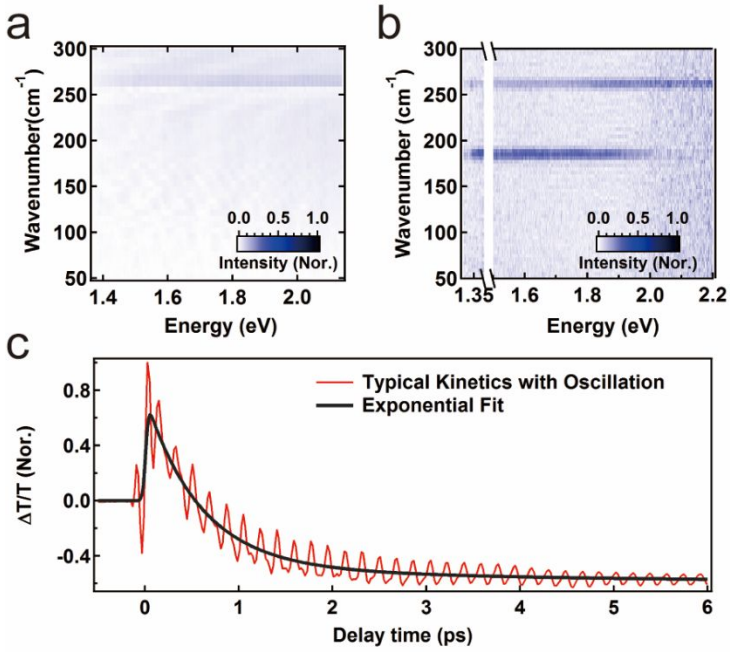

Fig. S7. (a) Associated probe energy-resolved Fourier-transformed map of chloroform solvent with oleylamine ligand. A weak solvent response mode can be observed at ~260 cm^{-1}. (b) Associated probe energy-resolved Fourier-transformed map of $SnSe_2$ NSs by 1.45eV Excitation. (c) Typical kinetics at 1.65 eV with oscillation and exponential fit.

SI7. Experimental details

Chemicals. Tin (IV) chloride pentahydrate ($SnCl_4 \cdot 5H_2O$, 98%), Selenium oxide (SeO_2, 99.9%), 1,10-phenanthroline ($C_{12}H_8N_2$, 99%) and oleylamine (OAM, 70%) were purchased from Sigma-Aldrich. Other common organic solvents (toluene, chloroform and so on, 99.5%) for sample purification and characterization were purchased from Sinopharm Chemical Reagent Co., Ltd. All chemicals were used as received without further purification.

$SnSe_2$ NSs Synthesis. In a typical synthesis, $SnCl_4 \cdot 5H_2O$ (35mg, 0.1 mmol), 1,10-phenanthroline (100 mg, 0.5 mmol), SeO_2 (22 mg, 0.2 mmol) were added into 10 mL OAM (~ 25 mmol) in a 25 mL three-neck flask. With Ar flow, after stirring for 5 min at room temperature, the mixture was heated up to 120℃ for 10 min then 200℃ for

20 h for reaction. The solution gradually turned dark and the black products were obtained. Varying the precursor ratio of Sn/Se (1:2, 1:3 and 1:4) by changing the amount of SeO_2 (22, 33 and 44 mg) can control the lateral size of $SnSe_2$ NSs. After reaction, the mixture was cooled down to 50℃, and about 4 times volume of toluene was added. The products were isolated by centrifuge and the precipitates were dispersed in toluene. This purification was repeated twice and the $SnSe_2$ NSs were finally dispersed in toluene or chloroform.

Characterizations. The $SnSe_2$ NSs were dropped onto an ultrathin carbon film on a copper grid for transmission electron microscopy (TEM) characterization. The TEM images were taken on a Hitachi 7700 transmission electron microscope at 100.0 kV. The selected area electron diffraction (SAED) and HRTEM images were taken on a JEM 2100F transmission electron microscope at 300.0 kV. The X-ray diffraction (XRD) patterns of $SnSe_2$ NSs were acquired on a Rigaku Ultimate-IV X-ray diffractometer. X-ray photoelectron spectroscopy (XPS) measurements were carried out on Thermo Scientific ESCALAB 250Xi XPS spectrometer. The thickness of $SnSe_2$ NSs was qualified by a Bruker Multimode 8 atomic force microscope (AFM). Raman spectrum was measured using home-build microscope with a 532 nm CW laser.

Density Functional Theory (DFT) Calculations. First-principles calculations were performed within the framework of density functional theory (DFT), as implemented in the Vienna *ab initio* simulation package (VASP)[2]. The exchange-correlation effects were treated using the Generalized Gradient Approximation (GGA) functional of Perdew, Burke and Ernzerhof[3] within the projector augmented wave

method[4]. The plane-wave basis set with a kinetic energy cutoff of 400 eV was used to expand the wave functions. The convergence thresholds for electronic and ionic relaxations were chosen to be 1.0×10^{-5} eV and 0.01 eV/ Å, respectively. The Brillouin zone was sampled using a Γ centered k-point schemes with a 12×12×8 grid mesh. DFT-D2 method[5] was employed to describe the interlayer van der Waals interactions. The electronic structures were calculated using a more accurate one-shot GW (G_0W_0) approach[6], where the involved total band number was about ten times larger than that of valence bands. The energy cutoff for the response function was set to be 150 eV. The maximally localized Wannier function[7], as implemented in the wannier90 package[8] was employed to interpolate the quasi-particle band structures of the G_0W_0 calculations, where p orbitals of Sn and Se atoms were chosen for the initial projections. In order to include the excitonic effects in optical spectra, the Bethe-Salpeter equation (BSE) calculations were carried out on top of the G_0W_0 method with the Tamm-Dancoff approximation[9].

Femtosecond Transient Absorption Measurement. $SnSe_2$ NSs dispersed in chloroform were loaded into 1mm quartz cuvette for transient absorption measurement. For femtosecond transient absorption spectroscopy (Time-Tech Spectra, TA100), the fundamental output from Yb:KGW laser (1030 nm, 220 fs Gaussian fit, 100 kHz, Light Conversion Ltd) was separated to two light beam. One was introduced to NOPA (ORPHEUS-N, Light Conversion Ltd) to produce a certain wavelength for pump beam, the other was focused onto a YAG plate to generate white light continuum as probe beam. The pump and probe overlapped on the sample at a small angle less than 10°.

The transmitted probe light from sample was collected by a linear array detector.

SI8. Transient absorption spectra and kinetics on exfoliated $SnSe_2$ flakes

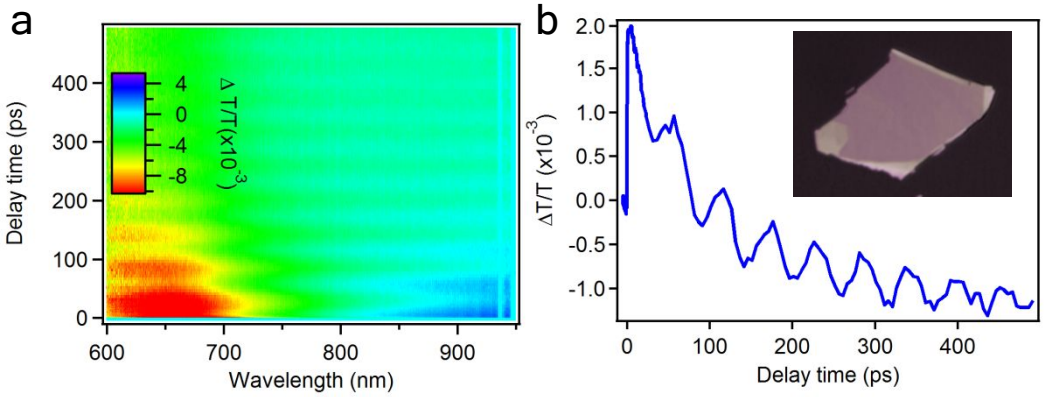

Fig. S8. (a) TA spectra of a representative exfoliated $SnSe_2$ flakes. (b) TA kinetics at 920nm. Inset: the optical image of measured flake.

Reference

1. Li L, C. Z., Hu Y, et al, Single-Layer Single-Crystalline SnSe Nanosheets. *J. Am. Chem. Soc.* **2013**, 135, 1213-1216.
2. Kresse, G.; Furthmüller, J., Efficient Iterative Schemes for ab initio Total-energy Calculations Using a Plane-wave Basis Set. *Phys. Rev. B* **1996,** *54*, 11169-11186.
3. Perdew, J. P.; Burke, K.; Ernzerhof, M., Generalized Gradient Approximation Made Simple. *Phys. Rev. Lett.* **1996,** *77*, 3865-3868.
4. Kresse, G.; Joubert, D., From Ultrasoft Pseudo Potentials to the Projector Augmented-wave Method. *Phys. Rev. B* **1999,** *59*, 1758-1775.
5. Grimme, S., Semiempirical GGA-type Density Functional Constructed with a Long-range Dispersion Correction. *J. Comput. Chem.* **2006,** *27*, 1787-99.
6. Shishkin, M.; Kresse, G., Implementation and Performance of the Frequency-dependent GW Method within the PAW Framework. *Phys. Rev. B* **2006,** *74*, 035101
7. Marzari, N.; Mostofi, A. A.; Yates, J. R.; Souza, I.; Vanderbilt, D., Maximally Localized Wannier Functions: Theory and Applications. *Rev. Mod. Phys.* **2012,** *84*, 1419-1475.
8. Mostofi, A. A.; Yates, J. R.; Pizzi, G.; Lee, Y.-S.; Souza, I.; Vanderbilt, D.; Marzari, N., An Updated Version of Wannier90: A Tool for Obtaining Maximally-localised Wannier Functions. *Comput. Phys. Commun.* **2014,** *185*, 2309-2310.
9. Paier, J.; Marsman, M.; Kresse, G., Dielectric Properties and Excitons for Extended Systems from Hybrid Functionals. *Phys. Rev. B* **2008,** *78*, 121201.